Acta Cryst C STRUCTURAL CHEMISTRY
ISSN 2053-2296

Structure and absolute configuration of natural fungal product beauveriolide I, isolated from *Cordyceps javanica*, determined by 3D electron diffraction

Kshitij Gurung,[a] Petr Šimek,[b] Alexandr Jegorov Jr[b] and Lukáš Palatinus[a]*

[a]Department of Structure Analysis, Institute of Physics of the Czech Academy of Sciences, Na Slovance 1999/2, Prague 8, 18221, Czech Republic, and [b]Biology Centre, Czech Academy of Sciences, Branišovská 1160/31, České Budějovice 2, 370 05, Czech Republic. *Correspondence e-mail: palat@fzu.cz

Received 21 December 2023
Accepted 11 February 2024

Keywords: crystal structure; natural product; 3D electron diffraction; absolute structure; Alzheimer's disease.

CCDC reference: 2332378

Supporting information: this article has supporting information at journals.iucr.org/c

Beauveriolides, including the main beauveriolide I {systematic name: (3*R*,6*S*,9*S*,13*S*)-9-benzyl-13-[(2*S*)-hexan-2-yl]-6-methyl-3-(2-methylpropyl)-1-oxa-4,7,10-triazacyclotridecane-2,5,8,11-tetrone, $C_{27}H_{41}N_3O_5$}, are a series of cyclodepsipeptides that have shown promising results in the treatment of Alzheimer's disease and in the prevention of foam cell formation in atherosclerosis. Their crystal structure studies have been difficult due to their tiny crystal size and fibre-like morphology, until now. Recent developments in 3D electron diffraction methodology have made it possible to accurately study the crystal structures of submicron crystals by overcoming the problems of beam sensitivity and dynamical scattering. In this study, the absolute structure of beauveriolide I was determined by 3D electron diffraction. The cyclodepsipeptide crystallizes in the space group *I*2 with lattice parameters a = 40.2744 (4), b = 5.0976 (5), c = 27.698 (4) Å and β = 105.729 (6)°. After dynamical refinement, its absolute structure was determined by comparing the R factors and calculating the z-scores of the two possible enantiomorphs of beauveriolide I.

1. Introduction

Beauveriolides represent a series of cyclodepsipeptides containing three amino acids and the unusual (3*S*,4*S*)-hydroxy-4-methylhydroxy acid. They were first described as beauveriolide metabolites of the entomopathogenic fungus *Beauveria bassiana* (Elsworth & Grove, 1977). Similar metabolites were further described in several other fungi of the genera Beauveria, Isaria or Paecilomyces (Kadlec *et al.*, 1994). The absolute configuration of the (3*S*,4*S*)-hydroxy acid component of beauveriolide I and II isolated from various Beauveria species was first estimated by synthesizing all possible chiral variants and comparing their ^{1}H and ^{13}C NMR spectra and optical rotation data (Mochizuki *et al.*, 1993). Recently, the beauveriolides (beauverolides) have attracted attention as potential drugs for the treatment of Alzheimer's disease and for preventing foam cell formation in atherosclerosis (Nagai *et al.*, 2008; Heneberg *et al.*, 2020). In particular, beauveriolide I (Fig. 1) has previously shown potent activity in inhibiting the formation of lipid droplets in mouse macrophages by specifically inhibiting the activity of acyl-coenzyme A (CoA):cholesterol acyltransferase (ACAT) (Namatame *et al.*, 2004; Tomoda & Doi, 2008). Inhibition of ACAT also reduces the secretion of amyloid-β peptide (Huttunen *et al.*, 2007; Puglielli *et al.*, 2001), the accumulation of which in brain *loci* is known to progress Alzheimer's disease (Hardy & Selkoe, 2002).

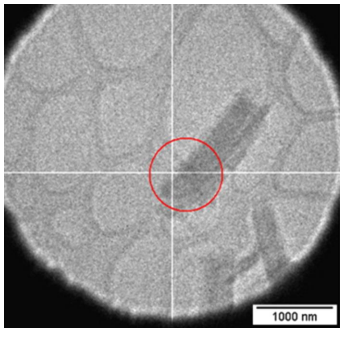

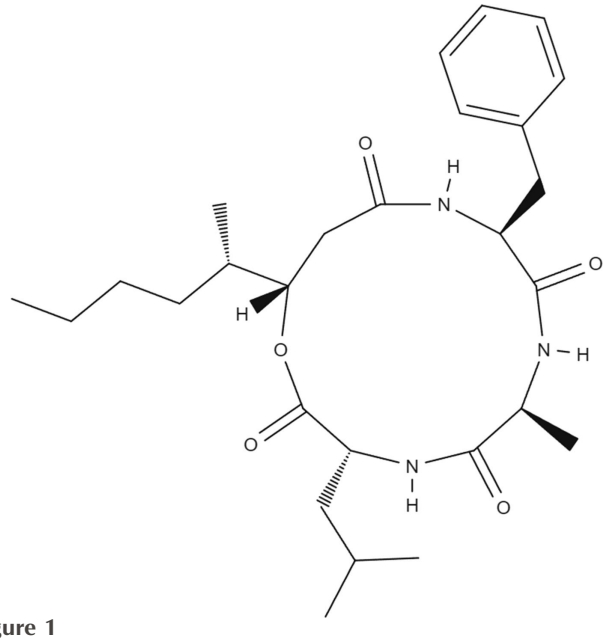

Figure 1
The molecular structure of beauveriolide I.

Beauveriolides form very small fibre-like crystals. Therefore, the determination of their single-crystal structure has never been successful, which, together with the difficulty of correctly identifying 3-hydroxy-4-methylhydroxy acid and its chirality led to probably identical metabolites from several fungi being described under different names. This ambiguity still exists today. The structure and conformation of beauveriolides remain important for understanding their physical properties, their role in the self–nonself recognition as fungal metabolites by the insect immune system, and for investigating their potential role in the treatment of human diseases.

In the last decade, thanks to the tremendous progress in data acquisition and processing, 3D electron diffraction (ED) has become an effective tool in crystallography for determining the structure of crystals of various compounds, including inorganics, organics, metal–organic frameworks (MOFS) and biological samples. The great advantage of 3D ED is that in a transmission electron microscope (TEM), very small crystals with a volume in the range of 10^{0} to 10^{-5} μm^{3} can be easily located, and the beam can be focused to perform ED measurements (Gemmi *et al.*, 2019). Continuous rotation electron diffraction (cRED) has become the most common data-acquisition technique in 3D ED, where a sample is continuously rotated over a range, while the diffraction data is collected at a certain tilt-step. Thus, cRED enables fast data collection, minimizing the electron dose on the sample, and making it very useful for beam-sensitive samples, including organic samples. The electrons used in 3D ED interact much more strongly than the more commonly used X-ray, resulting in multiple scattering of the beam, called dynamic scattering, and described by the dynamical theory of diffraction. The dynamical diffraction causes nonlinear deviations in the diffracted intensities from the kinematic limit. A technique called dynamical refinement (Palatinus *et al.*, 2015) takes these effects into account in the calculation of model intensities during structure refinement, giving more accurate and reliable results than those obtained without the application of the dynamical diffraction theory. In addition, the dynamical effects are sensitive to the absolute structure of noncentrosymmetric crystals (Spence *et al.*, 1994), enabling accurate structure determination and structure configuration of the crystals (Klar *et al.*, 2023; Brázda *et al.*, 2019).

In this study, we collected the 3D ED patterns of beauveriolide I using cRED experiments to solve its crystal structure. Despite the difficulties with the data quality resulting from the beam sensitivity of the crystal, we obtained satisfactory dynamical refinement, including the determination of absolute structure, thus confirming the absolute configuration of the chiral centres of beauveriolide I.

2. Experimental

2.1. Isolation of beauveriolide I

The surface stationary cultivation of *Cordyceps javanica* CCM8917 was carried out on a medium containing glucose (40 g), sorbitol (20 g), mannitol (10 g), soya peptone (30 g), KH_2PO_4 (1 g), $MgSO_4{\cdot}7H_2O$ (0.1 g), $ZnSO_4{\cdot}7H_2O$ (0.01 g) and water (1 l), for 18 d at 297 K. The isolated mycelium was washed with water and extracted several times with methanol (2 l). The extract was evaporated to dryness on a vacuum evaporator. HPLC–MS analysis revealed that the major isolated cyclodepsipeptide had characteristics of previously described beauveriolide I (Mochizuki *et al.*, 1993); the other beauveriolides were M, F, L and Q in an approximate ratio of 40:20:20:20 (% with respect to beauveriolide I as 100%). The crude mixture was purified first by column chromatography on silica gel with a stepwise gradient of dichloromethane/methanol. The final purification was carried out by preparative HPLC chromatography using a 354 mm × 18 mm internal diameter column, with Luna C8, 10 µm, and isocratic elution with methanol (85%) and water (15%). The crystalline material was obtained by the stepwise addition of water to the methanolic solution of beauveriolide I. Finally, the crystals were isolated by filtration and dried in air.

2.2. 3D electron diffraction (ED) experiment

The white powdery beauveriolide I sample was gently ground in an agate mortar. A TEM copper grid with holey carbon film was gently slid on the sample to stick some of the crystals onto the grid, and the excess was gently tapped off. The grid was loaded onto a cryo-holder and was inserted into an FEI Tecnai G2 20 TEM. The holder was then cooled to a temperature of 100 K before performing any measurements. The microscope was operated at 200 kV with a LaB_6 cathode, equipped with a Medipix 3 hybrid pixel detector ASI Cheetah (512 × 512 pixels, 24-bit dynamic range). The tilt step per frame was 0.3°, with the exposure time ranging from 504 to 1014 ms per frame. The crystals were found to be too sensitive to the electron beam to permit the collection of a full data set on a single crystal. Therefore, data sets from four different

crystals, labelled **a**–**d**, were merged to obtain a complete data set for the structure solution.

2.3. Data reduction and refinement

Indexation, lattice parameter determination and peak integration were performed using *PETS2* (Palatinus *et al.*, 2019). The processed data were imported into *JANA2020* (Petříček *et al.*, 2023) and the crystal structure was solved using *SHELXT* (Sheldrick, 2015). All non-H atoms were found in the solution. For the refinement, only crystals **b** and **c**, shown in Fig. 2, were used since the data from the other two crystals were very weak and yielded poor refinement *R* factors.

Detailed 3D ED set-up, crystal information and refinement details are given in Table 1.

3. Results and discussion

3.1. Structure solution and refinement

The crystal lattice of beauveriolide I was determined to be a body-centred monoclinic lattice with lattice parameters of a = 40.2744 (4), b = 5.0976 (5), c = 27.698 (4) Å and β = 105.729 (6)°. The reflection condition $h + k + l = 2n$ in the 2D reconstruction of reciprocal sections (Fig. S1 in the supporting information) indicates an *I*2 space group, which was further confirmed by the successful structure solution and refinement. There are two independent molecules in the asymmetric unit. The standard setting *C*2 was not used, because it leads to a very high monoclinic angle of 140.87°. Fig. S2 in the supporting information shows the structure of beauveriolide I down the *c* axis.

It can be observed clearly in Fig. 3(*a*) that one of the two molecules in an asymmetric unit has a distorted benzene ring with very large atomic displacement parameters (ADPs) for four C atoms (labelled C40, C41, C43 and C44 in Fig. 3). The electrostatic potential map after an initial dynamical refinement [Fig. 3(*b*)] shows the broadening of the potential around the C atoms. Therefore, to better model this benzene ring, the four C atoms along with their H atoms were split equally into two different positions [Fig. 3(*c*)]. The relative occupancy of the two positions was refined freely. Subsequent refinements led to significantly improved ADPs of these C atoms, as well as improved *R* factors.

The H atoms for all the C atoms were added to geometrically determined positions. These H atoms were refined with $U_{iso}(H) = 1.2U_{iso}(C)$. The C—H distances were fixed to 1.06 Å, *i.e.* to the internuclear distances, as electron diffraction does not suffer from the biased H-atom positions in the same way as X-ray diffraction data. To determine the arrangement of the H atoms bonded to the N atoms, initial dynamical refinement

Table 1
3D ED experimental, crystal structure and refinement details.

3D ED experimental information	
Collection method	Continuous-rotation data collection from four crystals
Tilt information	Crystal label α_{min}, α_{max}, $\Delta\alpha$ (°)
	a −34.38, 33.99, 0.30
	b −45.05, 16.06, 0.30
	c −44.43, 32.61, 0.30
	d −28.38, 10.60, 0.30
Exposure time (ms)	1014, 504, 504, 504
Beam diameter (nm)	960, 2150, 1050, 1050
Camera length (mm)	1500
Crystal information	
Empirical formula	$C_{27}H_{41}N_3O_5$
Z, Z'	8, 2
Space group	*I*2
a, b, c (Å)	40.2744 (4), 5.0976 (5), 27.698 (4)
α, β, γ (°)	90, 105.729 (6), 90
V (Å^3)	5473.63
Apparent mosaicities (°)	0.2765, 0.4080, 0.0598, 0.1323
Completeness (%)	100
Kinematical refinement	
sin (θ_{max})/λ (Å^{-1})	0.55
N_{obs}, N_{all}	3953, 6836
Parameters	298
R_{obs}, wR_{obs} (%)	18.39, 23.55
R_{all}, wR_{all} (%)	24.58, 25.38
min[$\Delta V(r)$], max[$\Delta V(r)$] (e Å^{-1})	−0.96, 1.00
Dynamical refinement	
sin (θ_{max})/λ (Å^{-1})	0.55
N_{obs}, N_{all}	5888, 14562
Parameters	365
R_{obs}, wR_{obs} (%)	11.73, 12.07
R_{all}, wR_{all} (%)	17.45, 12.82
min[$\Delta V(r)$], max[$\Delta V(r)$] (e Å^{-1})	−0.56, 0.53

Computer programs: *PETS2* (Palatinus *et al.*, 2019), *JANA2020* (Petříček *et al.*, 2023), *SHELXT* (Sheldrick, 2015) and *VESTA* (Momma & Izumi, 2008).

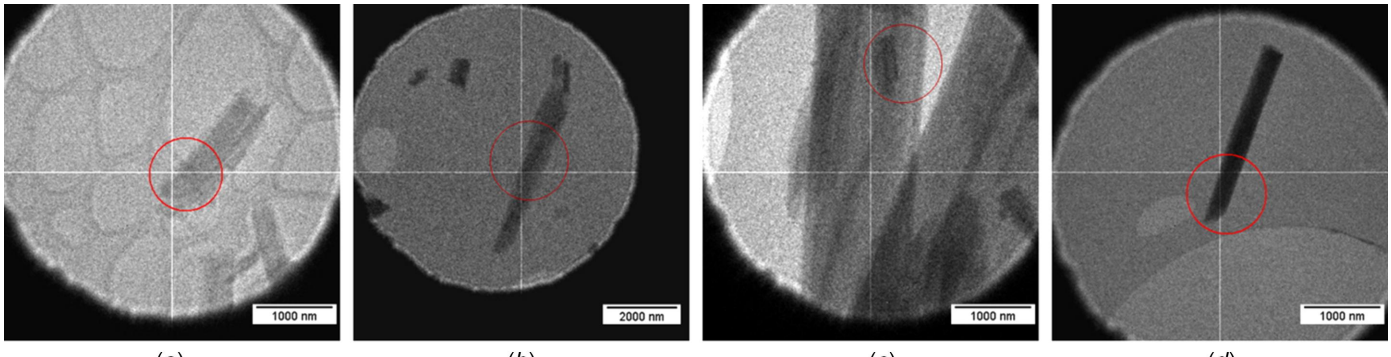

Figure 2
Crystals of beauveriolide I used for the 3D ED measurements. The red circles indicate the size of the illuminating electron beam.

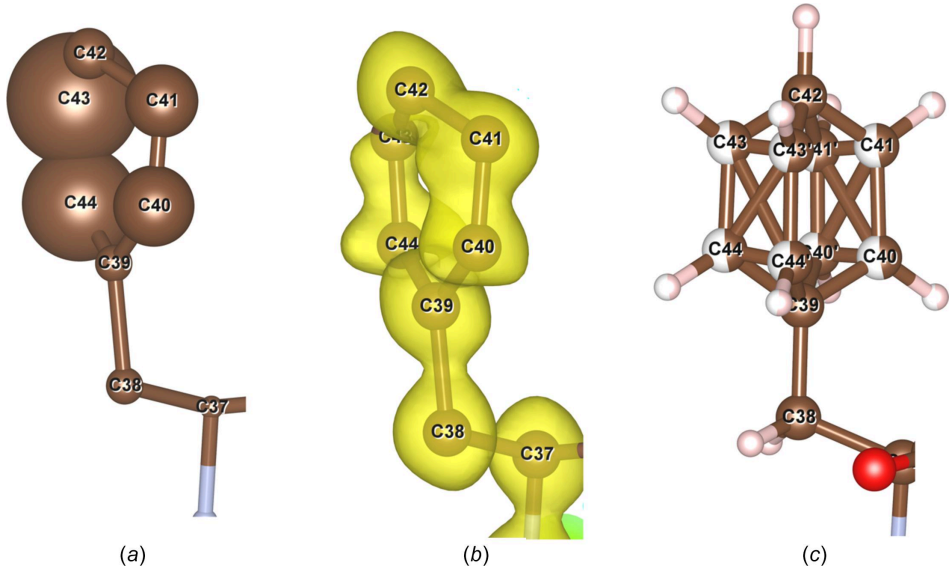

Figure 3
The benzene ring of one of the two asymmetric units of the solved beauveriolide I structure after an initial kinematical refinement, showing its distorted shape, together with (*a*) very high ADPs. (*b*) Fourier map showing four of the C atoms (C40, C41, C43 and C44) to be disordered. (*c*) The positions of the four C atoms and the bonded H atoms were split into two positions.

of the crystal structure was performed without the H atoms, and the difference electrostatic potential (DESP) map was calculated to attempt the localization of the H-atom positions (Fig. 4). The H-atom positions shown in Fig. 4 are in their expected positions that form trigonal planar geometry with the N atoms and the two adjacent C atoms. Of the six N atoms in the asymmetric unit, the H atoms of four of them (N1, N2, N4 and N5) are clearly visible, with a density maximum between the N atoms and their adjacent O atoms. The lack of visibility of the H atoms in the other two N atoms is likely due to the data quality, which in turn, is likely due to the electron-beam sensitivity of the samples. For the final refinement, each of the six H atoms on the amine N atoms was added and fixed in the geometrically expected positions, with N—H distances of 1.01 Å and $U_{iso}(H) = 1.2U_{iso}(N)$.

The final refined structure of beauveriolide I [Fig. 5(*a*)] shows the stacking of the same asymmetric units along the *b* axis. As can be seen in Figs. 5(*b*) and 5(*c*), the stacking is stabilized by three hydrogen bonds between two molecules. Regarding the distorted benzene ring, the split model

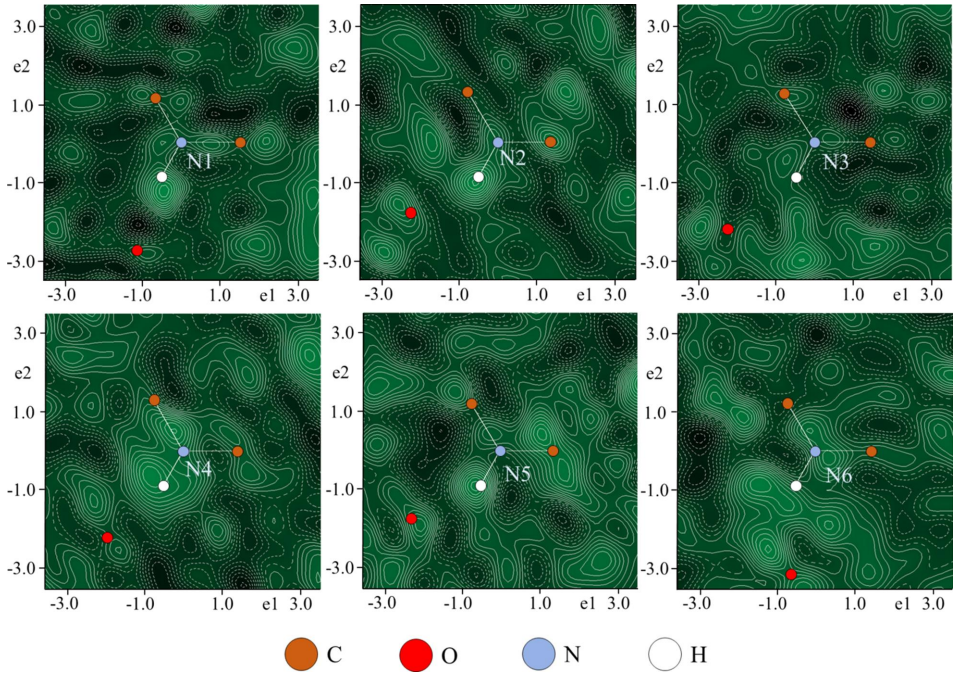

Figure 4
DESP maps in the C—N(H)—C planes of the two asymmetric units of the beauveriolide I structure. The black and green colours in the maps represent negative and positive contours, respectively, with a cutoff range of −0.561 to 0.751 e Å^{-1}. The H atoms displayed are at their expected positions.

considerably decreases the ADPs of the atoms. The split was found to be almost even, with an occupancy ratio of 0.47:0.53.

3.2. Determination of absolute configuration and absolute structure

Beauveriolide I is a chiral molecule and has two different enantiomers (Fig. 6), which can thus form two enantiomorphs in crystalline form. Structure models of both enantiomorphs were refined against the same data set using the same set of parameters and restraints. The correct absolute structure and configuration can be determined easily by comparing the refinement *R* factors (Table 2). The difference in the *R* factors is significant enough to point to 'Configuration A' as the correct enantiomer. To quantify the reliability of the absolute structure determination, we used the z-score method proposed by Klar *et al.* (2023). The z-score method provides the confidence level that the hypothesis that the selected configuration is correct. The z-score of 23.0σ for 'Configuration A' (Table 2) corresponds to a probability of correct absolute structure estimation indistinguishably close to 100%.

Table 2
Comparison of *R* factors and z-scores between the two enantiomorphs.

The z-scores were calculated assuming 'Configuration A' is the correct assignment.

	Configuration A	Configuration B
R_{obs}, wR_{obs} (%)	11.81, 12.16	15.21, 16.30
R_{all}, wR_{all} (%)	17.60, 12.91	20.96, 16.98
z-score from crystal **b** [Fig. 2(*b*)]	21.2σ	
z-score from crystal **c** [Fig. 2(*c*)]	10.0σ	
z-score from crystals **b** and **c** combined	23.0σ	

4. Conclusion

The crystal structure of beauveriolide I was solved *ab initio* using diffraction data collected from four crystals using

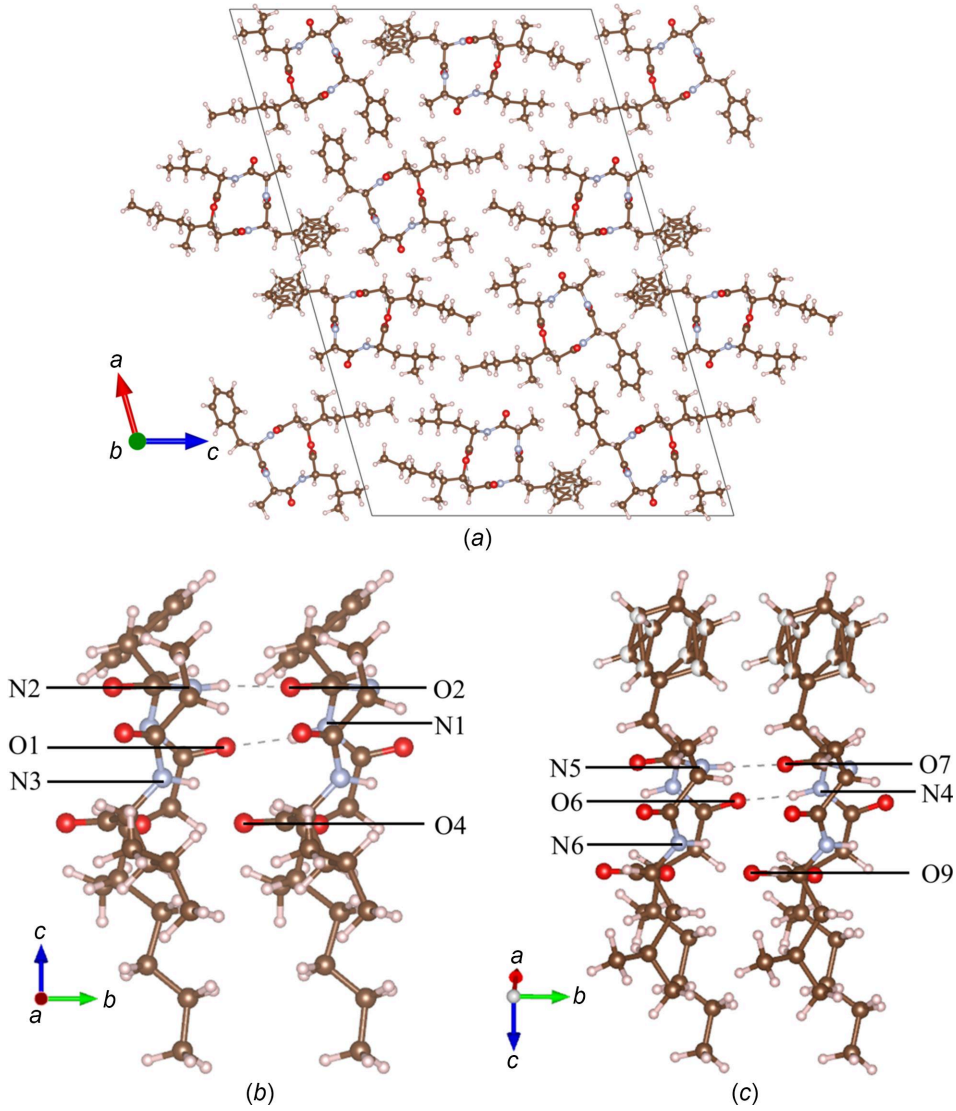

Figure 5
(*a*) A view of the crystal structure of beauveriolide I along the *b* axis after final dynamical refinement. (*b*)/(*c*) Hydrogen bonds stabilizing the stacking of the molecules along the *b* axis.

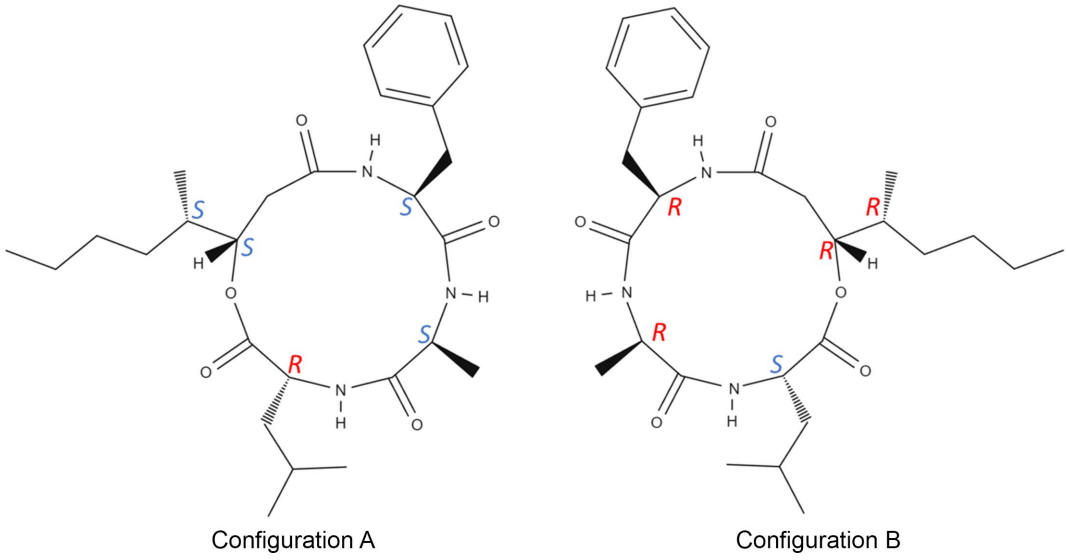

Figure 6
Enantiomers of beauveriolide I labelled 'Configuration A' and 'Configuration B' for simplicity. For each chiral C atom, their respective *R* and *S* configuration is labelled.

continuous-rotation 3D ED. The compound crystallized in the space group *I*2, with lattice parameters of a = 40.2744 (4), b = 5.0976 (5), c = 27.698 (4) Å and β = 105.729 (6)°. After the dynamical refinement of the solved structure without the H atoms in the amine groups, four out of six H atoms were located in the DESP maps, which were found to be in trigonal planar geometry, and the same case was assumed for the other two. The amine H atoms were found to form hydrogen bonds with the O atoms of adjacent molecules along the *b* axis. The absolute structure was determined using the z-score method at the confidence level of 23.0σ. This study, apart from providing the structure of the studied compound, further highlights the utility of the 3D ED technique for studying structures of complex beam-sensitive organic compounds, including natural products. The robustness of the absolute structure determination is an important feature of the method, which is of foremost importance in the analysis of natural products, where the absolute configuration is often unknown and difficult to determine.

Acknowledgements

The authors acknowledge the Czech Science Foundation and the Czech Technological Agency for funding the research. CzechNanoLab, funded by MEYS CR, is acknowledged for the financial support of the measurements at LNSM Research Infrastructure.

Funding information

The following funding is acknowledged: Grantov Agentura Česk Republiky (grant No. 21-05926X to L. Palatinus); Technologick Agentura Česk Republiky (grant No. SS0102045 to P. Šimek); Ministry of Education, Youth and Sports (project No. LM2023051). Open access publishing facilitated by Fyzikalni ustav Akademie ved Ceske republiky, as part of the Wiley-CzechELib agreement.

References

Brázda, P., Palatinus, L. & Babor, M. (2019). *Science*, **364**, 667–669.
Elsworth, J. F. & Grove, J. F. (1977). *J. Chem. Soc. Perkin Trans. 1*, pp. 270–273.
Gemmi, M., Mugnaioli, E., Gorelik, T. E., Kolb, U., Palatinus, L., Boullay, P., Hovmöller, S. & Abrahams, J. P. (2019). *ACS Cent. Sci.* **5**, 1315–1329.
Hardy, J. & Selkoe, D. J. (2002). *Science*, **297**, 353–356.
Heneberg, P., Jegorov, A. & Šimek, P. (2020). *CyTA J. Food*, **18**, 644–652.
Huttunen, H. J., Greco, C. & Kovacs, D. M. (2007). *FEBS Lett.* **581**, 1688–1692.
Kadlec, Z., Šimek, P., Heydová, A., Jegorov, A., Maťha, V., Landa, Z. & Eyal, J. (1994). *Biochem. Syst. Ecol.* **22**, 803–806.
Klar, P. B., Krysiak, Y., Xu, H., Steciuk, G., Cho, J., Zou, X. & Palatinus, L. (2023). *Nat. Chem.* **15**, 848–855.
Mochizuki, K., Ohmori, K., Tamura, H., Shizuri, Y., Nishiyama, S., Miyoshi, E. & Yamamura, S. (1993). *Bull. Chem. Soc. Jpn*, **66**, 3041–3046.
Momma, K. & Izumi, F. (2008). *J. Appl. Cryst.* **41**, 653–658.
Nagai, K., Doi, T., Ohshiro, T., Sunazuka, T., Tomoda, H., Takahashi, T. & Ōmura, S. (2008). *Bioorg. Med. Chem. Lett.* **18**, 4397–4400.
Namatame, I., Tomoda, H., Ishibashi, S. & Ōmura, S. (2004). *Proc. Natl Acad. Sci. USA*, **101**, 737–742.
Palatinus, L., Brázda, P., Jelínek, M., Hrdá, J., Steciuk, G. & Klementová, M. (2019). *Acta Cryst.* B**75**, 512–522.
Palatinus, L., Petříček, V. & Corrêa, C. A. (2015). *Acta Cryst.* A**71**, 235–244.
Petříček, V., Palatinus, L., Plášil, J. & Dušek, M. (2023). *Z. Kristallogr. Cryst. Mater.* **238**, 271–282.
Puglielli, L., Konopka, G., Pack-Chung, E., Ingano, L. A., Berezovska, O., Hyman, B. T., Chang, T. Y., Tanzi, R. E. & Kovacs, D. M. (2001). *Nat. Cell Biol.* **3**, 905–912.
Sheldrick, G. M. (2015). *Acta Cryst.* C**71**, 3–8.
Spence, J. C. H., Zuo, J. M., O'Keeffe, M., Marthinsen, K. & Hoier, R. (1994). *Acta Cryst.* A**50**, 647–650.
Tomoda, H. & Doi, T. (2008). *Acc. Chem. Res.* **41**, 32–39.

supporting information

Acta Cryst. (2024). C**80**, 56-61 [https://doi.org/10.1107/S2053229624001359]

Structure and absolute configuration of natural fungal product beauveriolide I, isolated from *Cordyceps javanica*, determined by 3D electron diffraction

Kshitij Gurung, Petr Šimek, Alexandr Jegorov and Lukáš Palatinus

Computing details

(3*R*,6*S*,9*S*,13*S*)-9-Benzyl-13-[(2*S*)-hexan-2-yl]-6-methyl-3-(2-methylpropyl)-1-oxa-4,7,10-triazacyclotridecane-2,5,8,11-tetrone

Crystal data

$C_{27}H_{41}N_3O_5$
M_r = 487.6
Monoclinic, *I*2
Hall symbol: I 2y
a = 40.2744 (4) Å
b = 5.0976 (5) Å
c = 27.698 (4) Å
β = 105.729 (6)°
V = 5473.6 (9) Å^3
Z = 8
F(000) = 2112

cell parameters determined from the combined data of four crystals
D_x = 1.184 Mg m^{-3}
Electrons 200 *K*eV radiation, *λ* = 0.0251 Å
Cell parameters from 13569 reflections
θ = 0.1–0.8°
μ = 0 mm^{-1}
T = 100 K
Long, flat rods, white
0.01 × 0.0004 × 0.0001 mm

Data collection

TEM FEI Tecnai G2 20 diffractometer
Radiation source: Lab6 cathode
continuous rotation 3D ED scans
15190 measured reflections
6694 independent reflections

4154 reflections with $I > 3\sigma(I)$
θ_{max} = 0.8°, θ_{min} = 0.1°
h = −27→27
k = −4→4
l = −24→24

Refinement

Refinement on *F*
$R[F^2 > 2\sigma(F^2)]$ = 0.110
$wR(F^2)$ = 0.120
S = 1.91
6694 reflections
364 parameters
6 restraints
370 constraints

H-atom parameters constrained
Weighting scheme based on measured s.u.'s $w = 1/(\sigma^2(F) + 0.0001F^2)$
$(\Delta/\sigma)_{max}$ = 0.052
$\Delta\rho_{max}$ = 0.16 e Å^{-3}
$\Delta\rho_{min}$ = −0.17 e Å^{-3}
Absolute structure: 3563 of Friedel pairs used in the refinement

Special details

Refinement. Structure refined by dynamical refinement. Hence, no R_int available. Dynamical refinement settings: gmax = 1.30 RSg = 0.70 DSg = 0.00 Nsteps = 150
Absolute structure determined by the z-score method (see Klar *et al.*, Nat. Chem. (2023), doi.org/10.1038/s41557-023-01186-1). The absolute structure is correct with the z-score level of 20.161.
Calculated intensities based on dynamical theory of electron diffraction. Number of individual data sets in refinement: 2 Block 1 refers to crystal #2 and block 2 refers to crystal #4 in the article. Block Thickness Nobs Nall Robs Rall wRall 1 1577.511 4154 6694 0.1098 0.1423 0.1199 2 1091.936 1733 7865 0.1351 0.2235 0.1555
Thickness given in Angstrom.
Refinement statistics relevant for the non-linear least-squares minimisation of wR(all): Number of reflections in refinement (obs/all): 5887 / 14559 Number of reflections present more than once: Number of reflections unique in point group 1: Robs: 0.1173 Rall: 0.1745 wRall: 0.1282
Post-refinement analysis of symmetrically-equivalent reflections: Number of unique reflections (obs/all): 3290 / 6246 MRobs: 0.1060 MRall: 0.1460 MwRall: 0.1104

Fractional atomic coordinates and isotropic or equivalent isotropic displacement parameters (Å²)

	x	*y*	*z*	U_{iso}*/U_{eq}	Occ. (<1)
C1	0.7101 (8)	−0.148 (6)	0.6294 (9)	0.366 (19)*	
C2	0.7024 (4)	−0.117 (4)	0.5728 (8)	0.175 (9)*	
C3	0.6990 (2)	−0.347 (2)	0.5370 (6)	0.046 (3)*	
C4	0.6924 (2)	−0.264 (2)	0.4804 (6)	0.026 (2)*	
C5	0.69465 (18)	−0.5085 (18)	0.4446 (4)	0.0098 (19)*	
C6	0.73089 (16)	−0.5961 (18)	0.4516 (4)	0.0094 (19)*	
C7	0.67521 (17)	−0.4504 (18)	0.3900 (4)	0.0028 (17)*	
C8	0.69023 (16)	−0.2136 (17)	0.3677 (4)	0.0034 (18)*	
C9	0.67215 (18)	−0.1430 (17)	0.3131 (4)	0.0037 (7)*	
C10	0.63663 (17)	−0.2819 (17)	0.2324 (4)	0.0041 (17)*	
C11	0.64427 (17)	−0.4551 (17)	0.1913 (4)	0.0053 (17)*	
C12	0.67936 (19)	−0.3984 (18)	0.1832 (4)	0.0059 (18)*	
C13	0.70758 (19)	−0.5479 (19)	0.2070 (4)	0.015 (2)*	
C14	0.7399 (2)	−0.4927 (18)	0.2017 (5)	0.020 (2)*	
C15	0.7450 (2)	−0.2846 (18)	0.1678 (5)	0.020 (2)*	
C16	0.7153 (2)	−0.149 (2)	0.1440 (5)	0.032 (3)*	
C17	0.6832 (2)	−0.1969 (18)	0.1500 (5)	0.013 (2)*	
C18	0.60048 (18)	−0.311492	0.2364 (4)	0.0037 (7)*	
C19	0.54926 (18)	−0.1095 (18)	0.2490 (4)	0.0090 (19)*	
C20	0.52102 (18)	−0.1650 (19)	0.2008 (4)	0.017 (2)*	
C21	0.54894 (18)	−0.3021 (18)	0.2903 (4)	0.0037 (7)*	
C22	0.5811 (2)	−0.4557 (19)	0.3758 (5)	0.013 (2)*	
C23	0.5785 (2)	−0.3392 (18)	0.4267 (5)	0.019 (2)*	
C24	0.5436 (2)	−0.224 (2)	0.4265 (5)	0.030 (3)*	
C25	0.5147 (2)	−0.432 (2)	0.4120 (5)	0.050 (3)*	
C26	0.5471 (3)	−0.103 (3)	0.4787 (7)	0.072 (4)*	
C27	0.61651 (17)	−0.5702 (18)	0.3823 (4)	0.0036 (18)*	
C28	0.3873 (3)	−0.530 (3)	0.4218 (6)	0.071 (4)*	
C29	0.4021 (3)	−0.478 (3)	0.3777 (5)	0.058 (4)*	
C30	0.4114 (2)	−0.707 (2)	0.3528 (6)	0.028 (3)*	
C31	0.42025 (18)	−0.6471 (18)	0.3016 (5)	0.012 (2)*	

C32	0.43055 (18)	−0.8917 (18)	0.2752 (4)	0.0056 (18)*	
C33	0.46719 (19)	−0.9700 (19)	0.3049 (4)	0.027 (2)*	
C34	0.42586 (18)	−0.8470 (17)	0.2197 (4)	0.0045 (18)*	
C35	0.44713 (18)	−0.6100 (19)	0.2075 (5)	0.011 (2)*	
C36	0.43994 (18)	−0.5505 (18)	0.1546 (4)	0.0037 (7)*	
C37	0.42691 (19)	−0.7079 (18)	0.0662 (4)	0.0081 (19)*	
C38	0.4451 (2)	−0.914 (2)	0.0417 (6)	0.025 (2)*	
C39	0.4418 (2)	−0.849 (2)	−0.0124 (5)	0.029 (3)*	
C40	0.4469 (4)	−0.583 (5)	−0.0247 (14)	0.059 (6)*	0.468 (5)
C40′	0.4707 (5)	−0.675 (4)	−0.0228 (12)	0.059 (6)*	0.532 (5)
C41	0.4441 (4)	−0.533 (6)	−0.0790 (12)	0.061 (6)*	0.468 (5)
C41′	0.4645 (6)	−0.635 (4)	−0.0745 (11)	0.061 (6)*	0.532 (5)
C42	0.4371 (3)	−0.730 (2)	−0.1135 (7)	0.065 (4)*	
C43	0.4322 (4)	−0.986 (5)	−0.1015 (13)	0.051 (5)*	0.468 (5)
C43′	0.4142 (5)	−0.876 (4)	−0.0990 (12)	0.051 (5)*	0.532 (5)
C44	0.4343 (4)	−1.057 (6)	−0.0504 (12)	0.059 (6)*	0.468 (5)
C44′	0.4169 (5)	−0.938 (4)	−0.0452 (12)	0.059 (6)*	0.532 (5)
C45	0.38801 (18)	−0.7443 (17)	0.0486 (4)	0.0037 (7)*	
C46	0.33201 (19)	−0.5376 (18)	0.0280 (4)	0.018 (2)*	
C47	0.3145 (2)	−0.600 (2)	−0.0208 (5)	0.033 (3)*	
C48	0.31997 (19)	−0.7207 (18)	0.0658 (4)	0.0037 (7)*	
C49	0.3326 (2)	−0.853 (2)	0.1535 (6)	0.036 (3)*	
C50	0.3179 (2)	−0.697 (3)	0.1929 (7)	0.050 (3)*	
C51	0.3145 (3)	−0.867 (3)	0.2433 (8)	0.088 (5)*	
C52	0.2855 (4)	−1.067 (3)	0.2308 (8)	0.160 (7)*	
C53	0.3131 (5)	−0.705 (4)	0.2888 (8)	0.190 (9)*	
C54	0.3681 (2)	−0.9732 (19)	0.1791 (5)	0.014 (2)*	
H1c1	0.730129	−0.01687	0.647237	0.4398*	
H2c1	0.68766	−0.105446	0.640828	0.4398*	
H3c1	0.718053	−0.343366	0.639439	0.4398*	
H1c2	0.68101	0.010901	0.559902	0.2101*	
H2c2	0.71921	0.02525	0.56437	0.2101*	
H1c3	0.721527	−0.464535	0.54779	0.0547*	
H2c3	0.678775	−0.471835	0.540805	0.0547*	
H1c4	0.667779	−0.174977	0.467856	0.0317*	
H2c4	0.710575	−0.119336	0.477368	0.0317*	
H1c5	0.681892	−0.671109	0.455357	0.0118*	
H1c6	0.743617	−0.464335	0.432921	0.0113*	
H2c6	0.743865	−0.599392	0.490356	0.0113*	
H3c6	0.73101	−0.786849	0.436385	0.0113*	
H1c7	0.67749	−0.624257	0.37013	0.0033*	
H1c8	0.716839	−0.245442	0.37156	0.0041*	
H2c8	0.690893	−0.046721	0.390742	0.0041*	
H1c10	0.640892	−0.089434	0.220911	0.0049*	
H1c11	0.642929	−0.655418	0.200869	0.0063*	
H2c11	0.62486	−0.426362	0.1572	0.0063*	
H1c13	0.704375	−0.707809	0.229805	0.0184*	
H1c14	0.761418	−0.602393	0.222347	0.0244*	

H1c15	0.769368	−0.241634	0.162044	0.0235*	
H1c16	0.717608	0.003823	0.119137	0.0379*	
H1c17	0.661588	−0.084829	0.130261	0.0155*	
H1c19	0.543632	0.077649	0.261476	0.0108*	
H1c20	0.525479	−0.350322	0.186319	0.0206*	
H2c20	0.496672	−0.166121	0.208591	0.0206*	
H3c20	0.521319	−0.017273	0.173975	0.0206*	
H1c22	0.562507	−0.607124	0.364904	0.0161*	
H1c23	0.597932	−0.195271	0.439107	0.0227*	
H2c23	0.585506	−0.48456	0.454993	0.0227*	
H1c24	0.536399	−0.075451	0.398799	0.0364*	
H1c25	0.505487	−0.44339	0.372349	0.06*	
H2c25	0.524527	−0.617118	0.42647	0.06*	
H3c25	0.494137	−0.377968	0.427104	0.06*	
H1c26	0.555851	−0.248189	0.506668	0.0863*	
H2c26	0.564996	0.053893	0.484761	0.0863*	
H3c26	0.522721	−0.031803	0.480588	0.0863*	
H1c28	0.360261	−0.501932	0.410543	0.0853*	
H2c28	0.392889	−0.726102	0.434266	0.0853*	
H3c28	0.398628	−0.399261	0.451452	0.0853*	
H1c29	0.423638	−0.351111	0.389107	0.0698*	
H2c29	0.384648	−0.359233	0.350953	0.0698*	
H1c30	0.432541	−0.803767	0.377521	0.0332*	
H2c30	0.391312	−0.847141	0.346598	0.0332*	
H1c31	0.440226	−0.505356	0.307747	0.0143*	
H2c31	0.399046	−0.551279	0.276765	0.0143*	
H1c32	0.41382	−1.051784	0.275588	0.0067*	
H1c33	0.484224	−0.810789	0.30552	0.0329*	
H2c33	0.467312	−1.0191	0.34216	0.0329*	
H3c33	0.475339	−1.134232	0.287615	0.0329*	
H1c34	0.434168	−1.022581	0.206124	0.0054*	
H1c35	0.442526	−0.441183	0.227113	0.0133*	
H2c35	0.47385	−0.647672	0.222356	0.0133*	
H1c37	0.434027	−0.518272	0.05682	0.0097*	
H1c38	0.434211	−1.101383	0.044084	0.0305*	
H2c38	0.47157	−0.923496	0.061623	0.0305*	
H1c40	0.452377	−0.431434	0.002602	0.0714*	0.468 (5)
H1c40′	0.491966	−0.598687	0.005013	0.0714*	0.532 (5)
H1c41	0.447663	−0.339874	−0.090777	0.0733*	0.468 (5)
H1c41′	0.482911	−0.517953	−0.085587	0.0733*	0.532 (5)
H1c42	0.435445	−0.683056	−0.151396	0.0775*	
H1c43	0.426788	−1.131803	−0.129882	0.0615*	0.468 (5)
H1c43′	0.392977	−0.952002	−0.126906	0.0615*	0.532 (5)
H1c44	0.430549	−1.253395	−0.040631	0.071*	0.468 (5)
H1c44′	0.397999	−1.056088	−0.035457	0.071*	0.532 (5)
H1c46	0.325045	−0.337101	0.028004	0.0215*	
H1c47	0.312572	−0.430703	−0.043679	0.0401*	
H2c47	0.328097	−0.748581	−0.03427	0.0401*	

H3c47	0.28945	−0.66795	−0.021943	0.0401*
H1c49	0.316285	−1.011557	0.137672	0.0436*
H1c50	0.293608	−0.614476	0.174459	0.0603*
H2c50	0.33303	−0.526633	0.204827	0.0603*
H1c51	0.338449	−0.966987	0.254183	0.1061*
H1c52	0.279216	−1.111876	0.192037	0.1917*
H2c52	0.293457	−1.23957	0.252019	0.1917*
H3c52	0.263498	−0.987793	0.239694	0.1917*
H1c53	0.291342	−0.579061	0.2791	0.2282*
H2c53	0.310947	−0.832473	0.318091	0.2282*
H3c53	0.335857	−0.591793	0.300928	0.2282*
H1n1	0.664554	−0.521306	0.29269	0.0112*
H1n2	0.593891	0.081297	0.236734	0.0077*
H1n3	0.585367	−0.086925	0.341875	0.0166*
H1n4	0.440643	−0.944115	0.132849	0.0181*
H1n5	0.380141	−0.356243	0.052138	0.0077*
H1n6	0.347286	−0.49891	0.126524	0.0265*
N1	0.65894 (17)	−0.3336 (17)	0.2819 (4)	0.0093 (17)*
N2	0.58336 (17)	−0.0953 (18)	0.2401 (4)	0.0064 (11)*
N3	0.57291 (18)	−0.2609 (18)	0.3359 (4)	0.0138 (18)*
N4	0.43647 (18)	−0.7580 (18)	0.1201 (4)	0.0151 (18)*
N5	0.36839 (16)	−0.5320 (16)	0.0439 (4)	0.0064 (11)*
N6	0.33473 (19)	−0.6701 (19)	0.1163 (5)	0.022 (2)*
O1	0.66891 (17)	0.0942 (17)	0.3029 (4)	0.0139 (17)*
O2	0.58823 (15)	−0.5401 (17)	0.2383 (4)	0.0048 (15)*
O3	0.52579 (16)	−0.4763 (16)	0.2876 (4)	0.0079 (15)*
O4	0.62285 (17)	−0.8021 (17)	0.3845 (4)	0.0119 (16)*
O5	0.63964 (16)	−0.3806 (17)	0.3860 (4)	0.0084 (16)*
O6	0.43864 (18)	−0.3203 (17)	0.1390 (4)	0.0130 (16)*
O7	0.37405 (19)	−0.9673 (18)	0.0434 (4)	0.0221 (19)*
O8	0.2984 (2)	−0.8851 (19)	0.0501 (5)	0.026 (2)*
O9	0.37337 (18)	−1.1960 (18)	0.1827 (4)	0.0189 (18)*
O10	0.39091 (16)	−0.7797 (17)	0.1974 (4)	0.0101 (16)*

Geometric parameters (Å, º)

C1—C2	1.52 (3)	C31—H1c31	1.06
C1—H1c1	1.06	C31—H2c31	1.06
C1—H2c1	1.06	C32—C33	1.535 (10)
C1—H3c1	1.06	C32—C34	1.513 (16)
C2—C3	1.52 (3)	C32—H1c32	1.06
C2—H1c2	1.06	C33—H1c33	1.06
C2—H2c2	1.06	C33—H2c33	1.06
C3—C4	1.57 (2)	C33—H3c33	1.06
C3—H1c3	1.06	C34—C35	1.570 (13)
C3—H2c3	1.06	C34—H1c34	1.06
C4—C5	1.611 (16)	C34—O10	1.418 (9)
C4—H1c4	1.06	C35—C36	1.448 (17)

C4—H2c4	1.06	C35—H1c35	1.06
C5—C6	1.488 (10)	C35—H2c35	1.06
C5—C7	1.532 (14)	C36—N4	1.406 (14)
C5—H1c5	1.06	C36—O6	1.247 (13)
C6—H1c6	1.06	C37—C38	1.540 (16)
C6—H2c6	1.06	C37—C45	1.521 (10)
C6—H3c6	1.06	C37—H1c37	1.06
C7—C8	1.551 (13)	C37—N4	1.462 (15)
C7—H1c7	1.06	C38—C39	1.50 (2)
C7—O5	1.451 (10)	C38—H1c38	1.06
C8—C9	1.532 (14)	C38—H2c38	1.06
C8—H1c8	1.06	C39—C40	1.43 (3)
C8—H2c8	1.06	C39—C40′	1.55 (3)
C9—N1	1.314 (13)	C39—C44	1.47 (3)
C9—O1	1.241 (13)	C39—C44′	1.24 (2)
C10—C11	1.538 (14)	C40—C40′	1.06 (3)
C10—C18	1.497 (11)	C40—C41	1.50 (5)
C10—H1c10	1.06	C40—H1c40	1.06
C10—N1	1.443 (13)	C40′—C41′	1.40 (4)
C11—C12	1.518 (12)	C40′—H1c40′	1.06
C11—H1c11	1.06	C41—C41′	0.95 (3)
C11—H2c11	1.06	C41—C42	1.36 (3)
C12—C13	1.379 (11)	C41—H1c41	1.06
C12—C17	1.413 (16)	C41′—C42	1.40 (3)
C13—C14	1.378 (13)	C41′—H1c41′	1.06
C13—H1c13	1.06	C42—C43	1.38 (3)
C14—C15	1.467 (16)	C42—C43′	1.33 (3)
C14—H1c14	1.06	C42—H1c42	1.06
C15—C16	1.382 (13)	C43—C43′	0.93 (3)
C15—H1c15	1.06	C43—C44	1.44 (5)
C16—C17	1.372 (14)	C43—H1c43	1.06
C16—H1c16	1.06	C43′—C44	1.65 (4)
C17—H1c17	1.06	C43′—C44′	1.50 (5)
C18—N2	1.319 (10)	C43′—H1c43′	1.06
C18—O2	1.272 (9)	C44—C44′	0.96 (3)
C19—C20	1.527 (12)	C44—H1c44	1.06
C19—C21	1.510 (15)	C44′—H1c44′	1.06
C19—H1c19	1.06	C45—N5	1.326 (11)
C19—N2	1.462 (12)	C45—O7	1.259 (12)
C20—H1c20	1.06	C46—C47	1.381 (15)
C20—H2c20	1.06	C46—C48	1.575 (16)
C20—H3c20	1.06	C46—H1c46	1.06
C21—N3	1.383 (13)	C46—N5	1.411 (10)
C21—O3	1.275 (11)	C47—H1c47	1.06
C22—C23	1.558 (18)	C47—H2c47	1.06
C22—C27	1.507 (11)	C47—H3c47	1.06
C22—H1c22	1.06	C48—N6	1.387 (16)
C22—N3	1.455 (15)	C48—O8	1.199 (12)

C23—C24	1.521 (13)	C49—C50	1.59 (2)
C23—H1c23	1.06	C49—C54	1.543 (12)
C23—H2c23	1.06	C49—H1c49	1.06
C24—C25	1.547 (14)	C49—N6	1.410 (18)
C24—C26	1.54 (2)	C50—C51	1.68 (3)
C24—H1c24	1.06	C50—H1c50	1.06
C25—H1c25	1.06	C50—H2c50	1.06
C25—H2c25	1.06	C51—C52	1.52 (2)
C25—H3c25	1.06	C51—C53	1.52 (3)
C26—H1c26	1.06	C51—H1c51	1.06
C26—H2c26	1.06	C52—H1c52	1.06
C26—H3c26	1.06	C52—H2c52	1.06
C27—O4	1.207 (12)	C52—H3c52	1.06
C27—O5	1.327 (11)	C53—H1c53	1.06
C28—C29	1.52 (2)	C53—H2c53	1.06
C28—H1c28	1.06	C53—H3c53	1.06
C28—H2c28	1.06	C54—O9	1.154 (13)
C28—H3c28	1.06	C54—O10	1.349 (12)
C29—C30	1.455 (18)	H1c40′—H1c40′^{i}	0.7703
C29—H1c29	1.06	H1n1—N1	1.01
C29—H2c29	1.06	H1n2—N2	1.01
C30—C31	1.58 (2)	H1n3—N3	1.01
C30—H1c30	1.06	H1n4—N4	1.01
C30—H2c30	1.06	H1n5—N5	1.01
C31—C32	1.558 (15)	H1n6—N6	1.01

C2—C1—H1c1	109.47	C35—C34—O10	104.8 (7)
C2—C1—H2c1	109.47	H1c34—C34—O10	114.89
C2—C1—H3c1	109.47	C34—C35—C36	114.1 (8)
H1c1—C1—H2c1	109.47	C34—C35—H1c35	109.47
H1c1—C1—H3c1	109.47	C34—C35—H2c35	109.47
H2c1—C1—H3c1	109.47	C36—C35—H1c35	109.47
C1—C2—C3	123.2 (19)	C36—C35—H2c35	109.47
C1—C2—H1c2	109.47	H1c35—C35—H2c35	104.42
C1—C2—H2c2	109.47	C35—C36—N4	119.1 (9)
C3—C2—H1c2	109.47	C35—C36—O6	121.7 (10)
C3—C2—H2c2	109.47	N4—C36—O6	119.1 (11)
H1c2—C2—H2c2	90.95	C38—C37—C45	110.3 (8)
C2—C3—C4	113.7 (12)	C38—C37—H1c37	108.82
C2—C3—H1c3	109.47	C38—C37—N4	107.8 (8)
C2—C3—H2c3	109.47	C45—C37—H1c37	110.89
C4—C3—H1c3	109.47	C45—C37—N4	105.6 (9)
C4—C3—H2c3	109.47	H1c37—C37—N4	113.3
H1c3—C3—H2c3	104.84	C37—C38—C39	111.3 (8)
C3—C4—C5	112.6 (9)	C37—C38—H1c38	109.47
C3—C4—H1c4	109.47	C37—C38—H2c38	109.47
C3—C4—H2c4	109.47	C39—C38—H1c38	109.47
C5—C4—H1c4	109.47	C39—C38—H2c38	109.47

C5—C4—H2c4	109.47	H1c38—C38—H2c38	107.58
H1c4—C4—H2c4	106.21	C38—C39—C40	117.9 (18)
C4—C5—C6	111.7 (7)	C38—C39—C40′	116.3 (13)
C4—C5—C7	111.1 (8)	C38—C39—C44	120.2 (15)
C4—C5—H1c5	108.52	C38—C39—C44′	119.0 (17)
C6—C5—C7	114.0 (9)	C40—C39—C40′	41.2 (11)
C6—C5—H1c5	105.2	C40—C39—C44	122 (2)
C7—C5—H1c5	105.82	C40—C39—C44′	108.3 (17)
C5—C6—H1c6	109.47	C40′—C39—C44	107.2 (17)
C5—C6—H2c6	109.47	C40′—C39—C44′	125 (2)
C5—C6—H3c6	109.47	C44—C39—C44′	40.7 (13)
H1c6—C6—H2c6	109.47	C39—C40—C40′	76 (2)
H1c6—C6—H3c6	109.47	C39—C40—C41	115 (2)
H2c6—C6—H3c6	109.47	C39—C40—H1c40	122.48
C5—C7—C8	113.2 (6)	C40′—C40—C41	87 (3)
C5—C7—H1c7	104.89	C40′—C40—H1c40	106.4
C5—C7—O5	110.6 (9)	C41—C40—H1c40	122.48
C8—C7—H1c7	110.26	C39—C40′—C40	63.2 (19)
C8—C7—O5	105.3 (7)	C39—C40′—C41′	109.9 (17)
H1c7—C7—O5	112.85	C39—C40′—H1c40′	125.04
C7—C8—C9	116.3 (6)	C40—C40′—C41′	89 (3)
C7—C8—H1c8	109.47	C40—C40′—H1c40′	114.38
C7—C8—H2c8	109.47	C41′—C40′—H1c40′	125.04
C9—C8—H1c8	109.47	C40—C41—C41′	87 (3)
C9—C8—H2c8	109.47	C40—C41—C42	122 (2)
H1c8—C8—H2c8	101.66	C40—C41—H1c41	119.12
C8—C9—N1	118.4 (8)	C41′—C41—C42	72 (2)
C8—C9—O1	116.5 (9)	C41′—C41—H1c41	111.38
N1—C9—O1	124.8 (10)	C42—C41—H1c41	119.12
C11—C10—C18	113.0 (7)	C40′—C41′—C41	97 (3)
C11—C10—H1c10	103.1	C40′—C41′—C42	128 (2)
C11—C10—N1	113.6 (7)	C40′—C41′—H1c41′	115.78
C18—C10—H1c10	110.82	C41—C41′—C42	67 (2)
C18—C10—N1	106.3 (9)	C41—C41′—H1c41′	107.51
H1c10—C10—N1	110.17	C42—C41′—H1c41′	115.78
C10—C11—C12	112.4 (7)	C41—C42—C41′	40.2 (12)
C10—C11—H1c11	109.47	C41—C42—C43	123 (2)
C10—C11—H2c11	109.47	C41—C42—C43′	103 (2)
C12—C11—H1c11	109.47	C41—C42—H1c42	118.49
C12—C11—H2c11	109.47	C41′—C42—C43	106.0 (17)
H1c11—C11—H2c11	106.32	C41′—C42—C43′	115 (2)
C11—C12—C13	120.2 (9)	C41′—C42—H1c42	120.8
C11—C12—C17	120.2 (7)	C43—C42—C43′	40.3 (13)
C13—C12—C17	119.5 (8)	C43—C42—H1c42	118.49
C12—C13—C14	121.0 (10)	C43′—C42—H1c42	124.14
C12—C13—H1c13	119.5	C42—C43—C43′	67 (2)
C14—C13—H1c13	119.5	C42—C43—C44	120 (3)
C13—C14—C15	121.1 (8)	C42—C43—H1c43	119.97

C13—C14—H1c14	119.46	C43′—C43—C44	85 (3)
C15—C14—H1c14	119.46	C43′—C43—H1c43	118.09
C14—C15—C16	114.5 (9)	C44—C43—H1c43	119.97
C14—C15—H1c15	122.76	C42—C43′—C43	73 (2)
C16—C15—H1c15	122.76	C42—C43′—C44	109.5 (15)
C15—C16—C17	125.1 (11)	C42—C43′—C44′	123.5 (19)
C15—C16—H1c16	117.47	C42—C43′—H1c43′	118.25
C17—C16—H1c16	117.46	C43—C43′—C44	60 (3)
C12—C17—C16	118.7 (8)	C43—C43′—C44′	96 (3)
C12—C17—H1c17	120.63	C43—C43′—H1c43′	102.28
C16—C17—H1c17	120.63	C44—C43′—C44′	35.3 (15)
C10—C18—N2	117.4 (5)	C44—C43′—H1c43′	120.68
C10—C18—O2	119.4 (6)	C44′—C43′—H1c43′	118.26
N2—C18—O2	123.1 (8)	C39—C44—C43	118 (2)
C20—C19—C21	112.6 (7)	C39—C44—C43′	98.2 (18)
C20—C19—H1c19	106.14	C39—C44—C44′	57 (2)
C20—C19—N2	111.9 (9)	C39—C44—H1c44	120.91
C21—C19—H1c19	106.93	C43—C44—C43′	34.3 (15)
C21—C19—N2	111.2 (7)	C43—C44—C44′	98 (3)
H1c19—C19—N2	107.72	C43—C44—H1c44	120.9
C19—C20—H1c20	109.47	C43′—C44—C44′	64 (3)
C19—C20—H2c20	109.47	C43′—C44—H1c44	131.71
C19—C20—H3c20	109.47	C44′—C44—H1c44	113.15
H1c20—C20—H2c20	109.47	C39—C44′—C43′	118 (2)
H1c20—C20—H3c20	109.47	C39—C44′—C44	82 (2)
H2c20—C20—H3c20	109.47	C39—C44′—H1c44′	120.79
C19—C21—N3	116.5 (8)	C43′—C44′—C44	81 (3)
C19—C21—O3	124.4 (8)	C43′—C44′—H1c44′	120.79
N3—C21—O3	118.5 (10)	C44—C44′—H1c44′	106.59
C23—C22—C27	109.4 (8)	C37—C45—N5	117.8 (7)
C23—C22—H1c22	108.68	C37—C45—O7	122.4 (8)
C23—C22—N3	111.7 (8)	N5—C45—O7	119.3 (7)
C27—C22—H1c22	108.9	C47—C46—C48	110.3 (8)
C27—C22—N3	111.5 (9)	C47—C46—H1c46	99.06
H1c22—C22—N3	106.51	C47—C46—N5	121.4 (10)
C22—C23—C24	115.6 (8)	C48—C46—H1c46	116.2
C22—C23—H1c23	109.47	C48—C46—N5	106.6 (8)
C22—C23—H2c23	109.47	H1c46—C46—N5	103.45
C24—C23—H1c23	109.47	C46—C47—H1c47	109.47
C24—C23—H2c23	109.47	C46—C47—H2c47	109.47
H1c23—C23—H2c23	102.62	C46—C47—H3c47	109.47
C23—C24—C25	111.5 (9)	H1c47—C47—H2c47	109.47
C23—C24—C26	107.6 (9)	H1c47—C47—H3c47	109.47
C23—C24—H1c24	110.56	H2c47—C47—H3c47	109.47
C25—C24—C26	112.8 (11)	C46—C48—N6	115.8 (8)
C25—C24—H1c24	105.17	C46—C48—O8	119.7 (11)
C26—C24—H1c24	109.25	N6—C48—O8	124.4 (12)
C24—C25—H1c25	109.47	C50—C49—C54	110.9 (10)

C24—C25—H2c25	109.47	C50—C49—H1c49	111.31
C24—C25—H3c25	109.47	C50—C49—N6	106.3 (10)
H1c25—C25—H2c25	109.47	C54—C49—H1c49	106.21
H1c25—C25—H3c25	109.47	C54—C49—N6	111.4 (9)
H2c25—C25—H3c25	109.47	H1c49—C49—N6	110.77
C24—C26—H1c26	109.47	C49—C50—C51	116.2 (10)
C24—C26—H2c26	109.47	C49—C50—H1c50	109.47
C24—C26—H3c26	109.47	C49—C50—H2c50	109.47
H1c26—C26—H2c26	109.47	C51—C50—H1c50	109.47
H1c26—C26—H3c26	109.47	C51—C50—H2c50	109.47
H2c26—C26—H3c26	109.47	H1c50—C50—H2c50	101.75
C22—C27—O4	124.5 (8)	C50—C51—C52	112.9 (14)
C22—C27—O5	110.5 (8)	C50—C51—C53	116.1 (13)
O4—C27—O5	125.1 (7)	C50—C51—H1c51	102.35
C29—C28—H1c28	109.47	C52—C51—C53	110.5 (17)
C29—C28—H2c28	109.47	C52—C51—H1c51	109
C29—C28—H3c28	109.47	C53—C51—H1c51	105.14
H1c28—C28—H2c28	109.47	C51—C52—H1c52	109.47
H1c28—C28—H3c28	109.47	C51—C52—H2c52	109.47
H2c28—C28—H3c28	109.47	C51—C52—H3c52	109.47
C28—C29—C30	116.6 (12)	H1c52—C52—H2c52	109.47
C28—C29—H1c29	109.47	H1c52—C52—H3c52	109.47
C28—C29—H2c29	109.47	H2c52—C52—H3c52	109.47
C30—C29—H1c29	109.47	C51—C53—H1c53	109.47
C30—C29—H2c29	109.47	C51—C53—H2c53	109.47
H1c29—C29—H2c29	101.23	C51—C53—H3c53	109.47
C29—C30—C31	114.9 (10)	H1c53—C53—H2c53	109.47
C29—C30—H1c30	109.47	H1c53—C53—H3c53	109.47
C29—C30—H2c30	109.47	H2c53—C53—H3c53	109.47
C31—C30—H1c30	109.47	C49—C54—O9	123.8 (8)
C31—C30—H2c30	109.47	C49—C54—O10	109.4 (8)
H1c30—C30—H2c30	103.42	O9—C54—O10	126.7 (8)
C30—C31—C32	114.9 (8)	C40′—H1c40′—H1c40′^{i}	109.27
C30—C31—H1c31	109.47	C9—N1—C10	121.8 (8)
C30—C31—H2c31	109.47	C9—N1—H1n1	119.11
C32—C31—H1c31	109.47	C10—N1—H1n1	119.11
C32—C31—H2c31	109.47	C18—N2—C19	120.5 (8)
H1c31—C31—H2c31	103.46	C18—N2—H1n2	119.77
C31—C32—C33	107.2 (7)	C19—N2—H1n2	119.77
C31—C32—C34	112.4 (8)	C21—N3—C22	123.2 (8)
C31—C32—H1c32	111.14	C21—N3—H1n3	118.38
C33—C32—C34	114.9 (8)	C22—N3—H1n3	118.38
C33—C32—H1c32	108.41	C36—N4—C37	120.8 (9)
C34—C32—H1c32	102.78	C36—N4—H1n4	119.58
C32—C33—H1c33	109.47	C37—N4—H1n4	119.58
C32—C33—H2c33	109.47	C45—N5—C46	123.7 (8)
C32—C33—H3c33	109.47	C45—N5—H1n5	118.15
H1c33—C33—H2c33	109.47	C46—N5—H1n5	118.15

H1c33—C33—H3c33	109.47	C48—N6—C49	121.4 (9)
H2c33—C33—H3c33	109.47	C48—N6—H1n6	119.31
C32—C34—C35	114.1 (8)	C49—N6—H1n6	119.31
C32—C34—H1c34	105.64	C7—O5—C27	119.0 (8)
C32—C34—O10	108.4 (8)	C34—O10—C54	118.7 (8)
C35—C34—H1c34	109.24		

Symmetry code: (i) −*x*+1, *y*, −*z*.

Hydrogen-bond geometry (Å, º)

D—H···*A*	*D*—H	H···*A*	*D*···*A*	*D*—H···*A*
C7—H1*c*7···O1^{ii}	1.06	2.30	3.307 (14)	157.79
C34—H1*c*34···O6^{ii}	1.06	2.44	3.422 (14)	152.90
C53—H2*c*53···C1^{iii}	1.06	2.47	3.50 (4)	164.01
C40′—H1*c*40′···C40^{i}	1.06	2.37	3.25 (2)	139.76
C40′—H1*c*40′···C40′^{i}	1.06	1.50	2.36 (3)	133.11
C40′—H1*c*40′···C41′^{i}	1.06	2.23	3.21 (3)	152.59
C41—H1*c*41···C43^{iv}	1.06	1.91	2.87 (4)	149.55
C41—H1*c*41···C44^{iv}	1.06	1.99	2.62 (4)	115.00
C42—H1*c*42···O2^{i}	1.06	2.45	3.46 (2)	160.70
C44—H1*c*44···C40^{ii}	1.06	1.82	2.79 (4)	150.40
C44—H1*c*44···C41^{ii}	1.06	1.94	2.62 (4)	118.30
N6—H1*n*6···O9^{iv}	1.01	2.24	3.178 (13)	153.52
N5—H1*n*5···O7^{iv}	1.01	2.00	2.888 (12)	144.65
N4—H1*n*4···O6^{ii}	1.01	1.93	2.910 (13)	163.26
N2—H1*n*2···O2^{iv}	1.01	1.95	2.838 (12)	145.88
N3—H1*n*3···O4^{iv}	1.01	2.19	3.139 (11)	155.17
N1—H1*n*1···O1^{ii}	1.01	1.98	2.980 (12)	169.65

Symmetry codes: (i) −*x*+1, *y*, −*z*; (ii) *x*, *y*−1, *z*; (iii) −*x*+1, *y*−1, −*z*+1; (iv) *x*, *y*+1, *z*.